USING CROSSINGS OF SATURN'S MAGNETOSPHERIC BOUNDARIES TO EXPLORE THE LINK BETWEEN UPSTREAM CONDITIONS AND RADIO EMISSION

C .M. Jackman[1]* , E. P. O'Dwyer[1] , C .K. Louis[1] ,
A. R. Fogg[1] , J. E. Waters[2] , and L. Lamy[3]

*Corresponding author: cjackman@cp.dias.ie

Abstract

Saturn has several components to its radio emission which can change in response to varying solar wind and magnetospheric conditions. These radio components include the Saturn Kilometric Radiation (SKR), a cyclotron maser instability-generated emission which occasionally displays Low Frequency Extensions (LFEs), some of which can last for more than a planetary rotation. We utilise a list of all magnetopause and bow shock crossings by Cassini during its 13-year tour of the Saturn system to explore how measurements of the upstream and near-boundary conditions at Saturn can inform our knowledge of the solar wind driving and its links to radio emission. Solar wind intervals give a direct measure of the upstream environment to compare against. Furthermore, bow shock and magnetopause crossings can be used in concert with boundary models to infer the upstream solar wind dynamic pressure at the time of crossings. We show several case studies which elucidate the timeline of solar wind–magnetosphere–ionosphere coupling at Saturn and outline open questions and future avenues for exploration.

---

[1] *School of Cosmic Physics, DIAS Dunsink Observatory, Dublin Institute for Advanced Studies (DIAS), Dublin 15, Ireland*

[2] *Department of Physics and Astronomy, University of Southampton, Highfield Campus, Southampton, SO17 1BJ, UK*

[3] *LAM, Pytheas, Aix Marseille Universite, CNRS, CNES, 38 Rue Frederic Joilot Curie, 13012 Marseille, France*

1   Introduction

Saturn's radio emissions were first sampled by the Voyager-1 spacecraft in 1980 (Kaiser et al., 1980), and our understanding of them significantly developed during the 13-year exploration of the near-Saturn system by the Cassini spacecraft which had a Radio and Plasma Wave Science (RPWS) instrument on board (Gurnett et al., 2004). The strongest component of Saturn's radio emissions is called the Saturn Kilometric Radiation (SKR), a cyclotron maser instability (CMI)–generated emission with a spectrum extending from $\sim$ 2 kHz to 1.2 MHz, and a broad peak generally located between $\sim$ 100 to 400 kHz. This emission is highly circularly/elliptically polarized which facilitates its identification among other kronian or solar radio emissions (e.g., Kaiser & Desch, 1984; Lamy et al., 2008a; Lamy, 2017).

It has long been postulated that there is a link between Saturn's radio emissions and the upstream solar wind conditions. Studies with Voyager data found a correlation between SKR intensity and solar wind dynamic pressure (Desch, 1982; Desch & Rucker, 1983) while more recent work with Cassini showed that the solar wind speed can be correlated with the period of the SKR (Zarka et al., 2007). A statistical study which compared various upstream parameters to SKR intensity found the strongest correlation with solar wind dynamic pressure (Taubenschuss et al., 2006). It appears there can be a finite lag between a change in upstream conditions and a response from the SKR. This response can take the form of (i) an intensification of the emission (Jackman et al., 2005b; Thomsen et al., 2019; Cecconi et al., 2022), (ii) a change in the regular pulsing of the emission (Badman et al., 2008), (iii) a change in the morphology of the emission, specifically an extension of the emission to lower frequencies (Bunce et al., 2005; Jackman et al., 2009; Reed et al., 2018). These so-called Low Frequency Extensions (LFEs) are interpreted as a growth/movement of the radio sources to higher altitudes along field lines, with the consequence of lower frequency emission being observed. LFEs are thought to be driven by solar wind compressions and also linked to dramatic magnetotail reconfiguration events which increase the precipitation of energetic particles into the auroral zone. LFEs have a well-studied terrestrial analogue in the extension of Auroral Kilometric Radiation (AKR) emission at Earth (Morioka et al., 2007). Dedicated missions like FAST have flown at low altitudes enabling direct examination of the auroral acceleration region and the location of radio sources (Ergun et al., 1998), which have been seen at altitude ranges of $\sim 1.8 - 3\ R_{\mathrm{E}}$ (Calvert, 1981). Future work will constrain the analogous altitude ranges at Saturn.

One of the main challenges at the outer planets is the lack of an upstream monitor to provide context for magnetospheric observations. At Saturn we have a rich dataset of 13 years of quasi-continuous radio observations from the Cassini spacecraft which bring potential to probe the site of particle acceleration and to act as a remote proxy for conditions which drive dynamics in the magnetosphere (e.g., Rucker et al., 2008). In this work we pursue several approaches to quantifying the link between the upstream solar wind conditions and Saturn's radio response. In Section 2 we introduce the data set and associated visibility constraints, in Section 3 we examine direct and indirect methods for exploring solar wind–radio connection. Section 4 presents a summary and future perspectives.

2 Dataset and visibility constraints

The Cassini spacecraft orbited Saturn from July 2004 to September 2017, and the Cassini Radio Plasma Wave Science (RPWS) High Frequency Receiver (HFR) took data quasi-continuously for this time, recording radio electric signals from 3.5 kHz to 16 MHz using two or three electric antennas with various operation modes affecting the time–frequency coverage (Gurnett et al., 2004). Goniopolarimetric inversions of 2- and 3-antenna measurements then provided the wave Stokes parameters, including the flux density S and the degree of circular polarization V. This instrument allows for reconstruction of the absolute flux density and polarisation of the observed radio waves (Cecconi & Zarka, 2005). For the purpose of analyzing solely the SKR component on long timescales, Lamy et al. (2008a) constructed a cleaned calibrated dataset made of regular time–frequency arrays for the quantities S (expressed in $W/m^2/Hz$ and normalized to 1 AU) and V ($= \pm 1$ for purely LH/RH circularly polarized waves). These arrays consist of 48 frequency channels (24 logarithmically spaced channels between 3.5 and 300 kHz and 24 linearly spaced channels between 350 and 1500 kHz) with a native time resolution of 180 s. For the purpose of this study, we used an updated version of this dataset with a time resolution of 90 s.

In addition to the remotely sensed radio emission, in this work we also employ data from the Cassini magnetometer instrument (Dougherty et al., 2004) and the Cassini Plasma Spectrometer (CAPS) (Young et al., 2004) (where available). During Cassini's excursions outside the magnetosphere, these datasets describe the Interplanetary Magnetic Field (IMF) and solar wind plasma parameters. These data were used by Jackman et al. (2019) to determine the timing of magnetopause and bow shock crossings during the Cassini mission. Boundary crossings were characterised by sharp changes in the character of field (amplitude, level of fluctuation, orientation), and plasma (density, temperature) properties, and the intervals in between magnetopause and bow shock crossings represent a significant amount of time spent in Saturn's turbulent magnetosheath. This boundary crossing list has since been updated with minor corrections and the full set of 2118 magnetopause and 1247 bow shock crossings is available here: Jackman (2022). In this work, we combine the boundary crossing times with models of the magnetopause (Kanani et al., 2010) and bow shock (Went et al., 2011) to infer the upstream solar wind dynamic pressure at the times of crossings by tracking back to the nose standoff distance. These dynamic pressure values give an instantaneous snapshot of conditions without the ability to account for rapid boundary motion.

2.1 Spacecraft coverage

Figure 1 shows the trajectory of the Cassini spacecraft from Saturn Orbit Insertion (SOI) in July 2004 to mission end in September 2017. Cassini's initial approach to Saturn was from the dawn flank and the first long capture orbit was also out towards dawn, with subsequent orbits covering all local times and a wide range of latitudes. There are magnetopause and bow shock crossings near the nose, and dawn/dusk flanks, and this diverse local time coverage is critical for comparing the viewing of radio sources from different observation points.
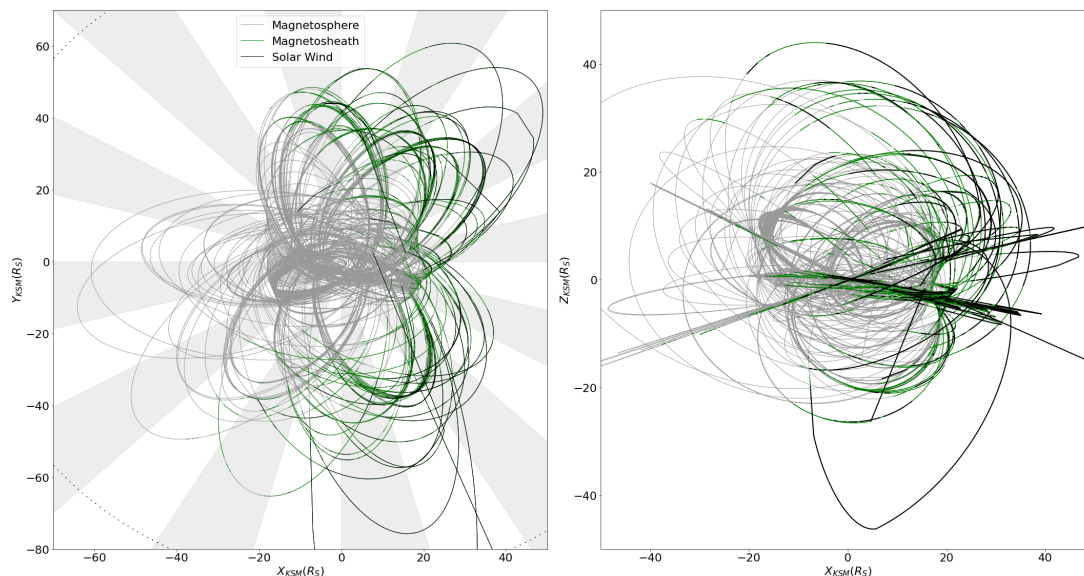
Figure 1: *Trajectory of the Cassini spacecraft from Saturn Orbit Insertion in July 2004 to mission end in September 2017. The grey lines show the trajectory within the magnetosphere, green within the magnetosheath, and black in the solar wind. Data are shown in the Kronian Solar Magnetospheric (KSM) co-ordinate system, where the x axis coincides with the direction of the Sun, the x-z plane contains the planetary dipole axis, and the y component is azimuthal, positive toward dusk. The left panel shows the x-y KSM view, and the right panel shows the x-z KSM view. Alternating grey and white markings in the left panel denote hour-wide local time sectors. Concentric dotted circles are drawn every 10 R_S.*

2.2 Visibility of Saturn's radio sources

Before interpreting any observed radio emissions, it is critical to take the viewing conditions into account. As mentioned above, SKR is CMI-generated, and it is beamed in hollow cones from source regions near the auroral zone. Previous studies at Saturn (Lamy et al., 2008b; Cecconi et al., 2009; Lamy et al., 2009; Kimura et al., 2013; Reed et al., 2018; Nakamura et al., 2019) have shown that the beamed nature of CMI-generated radio emissions and the constrained radio source locations results in emission which is preferentially observed from restricted sectors in local time and latitude. At Saturn, goniopolarimetric studies have revealed the typical location of radio sources in the morning–to–noon sector at high latitudes (Warwick et al., 1981; Lecacheux & Genova, 1983; Galopeau et al., 1995). In practice, this means that the most intense radio powers are observed whenever the most intense radio sources can be observed, typically from a two-peak window in Local Time separated from the source flux tube by several hours LT (Cecconi et al., 2009; Andrews et al., 2010; Lamy et al., 2013).

In addition to viewing constraints associated with the local time of the observer, there are also latitudinal influences on the measured radio signal. Lamy et al. (2008b) showed that the SKR spectrum maximizes whenever observed from $20-30^o$ latitude, while extinctions at both highest and lowest frequencies are seen from very high latitudes. Such features are correctly reproduced from simulations. Nakamura et al. (2019) examined the full Cassini near-Saturn dataset from 2004 to 2017, including occurrence distributions of the northern and southern SKR as a function of latitude. Close examination of these data reveals the extinction of the main SKR emission at higher latitudes as well as some hemispheric

Table 1: *Table of solar wind excursions with duration greater than 10 days following first Cassini capture orbit. Dates and times are given in the format YYYY-DOY-HR:MM (where DOY = Day of Year). Comments regarding each excursion are given in the right-hand column. The spacecraft is within 5° of the equatorial plane for all but the final solar wind excursion in 2016 when higher latitudes of 35° were reached.*

Start SW excursion	End SW excursion	Duration (days)	LT range (hrs)	Comment
2004-314-12:43	2004-345-09:07	32.75	5.5 - 8.5	Case study in Figure 2
2005-027-16:13	2005-042-07:52	14.50	6.5 - 8.3	2 moderate compressions with closely-associated LFEs
2007-205-02:00	2007-232-08:30	27.25	13 - 16	1 moderate compression with broad IMF amplitude increase and closely-associated LFE
2007-245-12:30	2007-265-18:25	20.25	12.9 - 15.8	Rarefaction and significant data gap
2007-301-22:30	2007-314-01:40	12.25	12.6 - 14.8	1 very broad compression signature with LFE activity throughout
2011-137-17:45	2011-151-21:46	14.25	14.5 - 16.1	1 clear compression preceded by LFE
2016-140-17:45	2016-152-14:24	11.75	6.9 - 9.8	Rarefaction and patchy radio emission observed from higher latitudes (approx 35°)

asymmetries. O'Dwyer et al. (2023) manually labelled hundreds of LFEs from the Cassini dataset and note a specific class of events called "extinction LFEs" which are observed from higher latitudes and where the upper frequency range of the main SKR band (around 400 to 600 kHz) is significantly attenuated and sometimes completely disappears when observed from the highest latitudes. Lamy et al. (2023) present a complete statistical examination of the Cassini dataset with a view to further characterising the SKR visibility as a function of the sub-observer co-ordinates (LT and latitude).

Thus clearly it is critical to take spacecraft location into consideration when interpreting both the signal strength and the frequency span of radio emissions at Saturn as it's possible to see attenuation across the spectrum, extinction of a portion of the spectrum, or reflection and refraction effects. For the short interval case studies presented in this work, viewing conditions are relatively steady as the spacecraft doesn't move much within the observation window. For bigger statistical studies which may follow from this work, where authors seek to quantitatively compare integrated powers and spectral morphologies across the mission, care should be taken to account for visibility effects.

3 Radio response to solar wind driving

There are several key ways in which we can assess the response of Saturn's radio emissions to external driving by the variable solar wind. Here we focus first (Section 3.1) on direct solar wind comparison with radio emission (tracking radio emissions while Cassini was outside the bow shock). We then follow up with an indirect examination (Section 3.2), inferring the upstream dynamic pressure at boundary crossings and tracking the radio signatures around those encounters.

3.1 Directly sampling solar wind

In the absence of an upstream monitor at Saturn, and given the uncertainties in shock arrival times from heliospheric propagation models, the most robust way to compare the upstream solar wind driver and the resultant planetary radio emission is by direct measurement of both simultaneously. Detailed studies of the IMF structure and solar wind properties upstream of Saturn during the Cassini approach phase and SOI capture orbit have been made (Jackman et al., 2004, 2005a), and compression intervals shown to elicit a response from the planet's radio emissions (Jackman et al., 2005b). Moreover, Taubenschuss et al. (2006) took a quantitative approach to examining the time lag between changes in upstream parameters and Saturn's radio response, basing their study on Cassini's approach to the planet prior to SOI as well as the first long capture orbit (2004 DOY 202 to 326: July 20th – November 21st).

For this study we focus on later data, beyond the first capture orbit. During its 13-year Saturn orbital tour, Cassini crossed the bow shock outbound and sampled the solar wind on a total of 623 occasions (Jackman et al., 2019; Jackman, 2022). The solar wind excursions vary in duration from several minutes to tens of days. Based on the duration of a solar rotation as seen from ~ 9 AU (25.5 days), and the typical phasing of compressions and rarefactions seen at Saturn orbit (two several-day long compressions each solar rotation, particularly during the declining phase of the solar cycle), we expect that 10 days or greater is a well justified time window of solar wind excursion to search for in the dataset to maximise the chances of capturing significant solar wind dynamics in the form of compressions. Table 1 shows the seven $\geq$ 10-day long solar wind excursions which the Cassini spacecraft made during its primary orbital tour of Saturn. As can be seen, these excursions from one outbound bow shock crossing to the next inbound crossing, range in duration from 11.75 to 32.75 days. Unfortunately, due to spacecraft pointing issues and an instrument failure in 2012, we do not have regular plasma measurements in the solar wind near Saturn so we cannot routinely measure parameters such as density, temperature, or solar wind dynamic pressure. For the solar wind excursions in this study we thus use magnetometer measurements as our primary indicator of the timing of solar wind compression. We manually inspected the IMF traces in all cases and noted compressions as the onset of intervals where the IMF magnitude exceeds 0.5 nT. We expect these compressions to be phased twice per solar rotation during the declining phase of the solar cycle (early years of Cassini Saturn exploration).

Figure 2 shows data from 2004 day 334-344 (November 29th – December 9th). This

10-day interval is part of a longer 32-day solar wind excursion. During the first 20 days of the excursion, the radio emission displayed regular SKR bursts modulated in concert with the Planetary Period Oscillations (PPOs) and the solar wind was relatively quiet (Bradley et al., 2020). The interval we discuss here reveals a significant departure from this steady state. During these 10 days, the spacecraft was inbound toward Saturn from its apoapsis position, traversing radial distances from ~ 72 to ~ 48 R_S on the dawn flank of the magnetosphere.
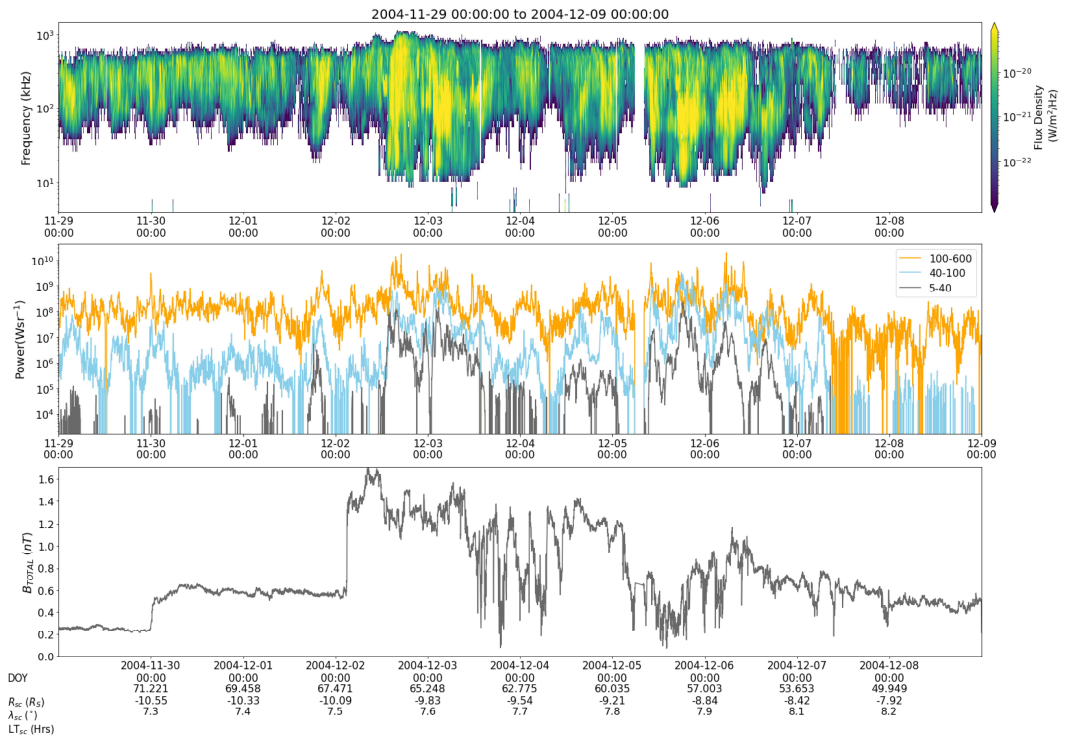
Figure 2: *10 days of Cassini radio and magnetometer data for an interval from 2004 day 334-344 (November 29th – December 9th). Top panel is a frequency–time spectrogram from Cassini RPWS, middle panel is the integrated radio power in 3 bands (100-600 kHz gold, 40-100 kHz blue, 5-40 kHz grey). The bottom panel shows the total IMF strength measured by Cassini in the solar wind.*

We observe a weak compression begin on November 30th with a small step change in the IMF magnitude. Three days later, on December 2nd at 03:00, we observe a much more significant sharp change in the amplitude of the field, representative of the arrival of a strong shock compression at the spacecraft, with an almost instantaneous increase in IMF magnitude of ~ 1 nT, consistent with the type of solar wind compressions reported in Jackman et al. (2004). Approximately 10 hours later the radio emissions start to significantly brighten and then explosively expand into a huge LFE which continues for almost 24 hours. We class this as a "monster LFE" such as those labelled by O'Dwyer et al. (2023). Such radio signatures are relatively rare, and are distinct from the more regular, short (few-hour) LFEs which tend to fall in phase with the PPOs (Badman et al., 2008; Reed et al., 2018). However, it can also be the case that long (> 1 planetary

rotation) LFEs (such as the one displayed here) are associated with the PPO systems. This phenomenon was examined in detail by Bradley et al. (2020) who noted that such LFEs can be associated with strong field-aligned currents initiated at thin plasma sheet phases where the magnetosphere becomes unstable to reconnection and significant energetic nightside particle injections can be initiated. We thus interpret this interval of severe radio disturbance as being directly driven by the arrival of a solar wind compression which in turn set in motion a chain of magnetospheric disturbance, culminating in the precipitation of energetic particles into the auroral zone, and the stimulation of radio sources at higher altitudes, producing the observed lower frequency radio emission. The timing of the appearance of the "monster LFE", in this case ~ 10 hours after the compression was observed upstream of the planet, may simply be related to the timing of the next favourable PPO cycle. Future statistical analyses of a comprehensive catalogue of LFEs from the full Cassini mission will unveil the complete detail of the link between LFEs and PPOs and any fundamental differences between short and long LFEs in terms of their drivers, and links to global magnetospheric dynamics.

It is very important to note that this is a favourable case study example. It had been hoped that solar wind excursions during the main Cassini mission may have yielded more opportunities to sample significant solar wind compressions in situ with field and plasma instruments and explore their radio counterparts. However, as can be seen from the notes in Table 1, many of the extended solar wind excursions did not lend themselves to such comparison. There are several reasons for this. Firstly, some intervals were hampered by data gaps. Secondly, several intervals displayed some moderate compressions but with very broad signatures in IMF magnitude, thus not allowing us to ascertain a clear start time for the effect of the compression. The sharp forward shocks such as shown in Figure 2 are somewhat exceptional. Thirdly, Cassini was a magnetospheric orbiter, with science goals which required much of its orbit to take place quite close to Saturn and its moons and rings. Thus the apoapses of the spacecraft during the main mission were all typically within 70 R_S of the planet with many within 40 R_S, particularly later in the mission as the spacecraft latitude increased. For the spacecraft to be sampling the solar wind at such positions, one would require a significantly compressed bow shock such that the boundary was pushed planetward of the spacecraft. Jackman et al. (2019) showed a distribution of inferred dynamic pressure from bow shock crossings made by Cassini compared to a distribution of dynamic pressure from a propagated model, and it revealed a clear shift of the bow shock crossing distribution to higher (more compressed) dynamic pressures. Thus it may be the case that when Cassini spent a significant amount of time in the solar wind near apoapsis, the primary compression which led to that scenario happened before the solar wind excursion, and thus the solar wind sampling revealed moderate or seemingly steady state conditions. We can postulate that compressions preceded these intervals, but with a single spacecraft the separation of temporal from spatial effects is extremely challenging and relies on several assumptions.

3.2 Inferring solar wind conditions near boundaries

As mentioned above, Cassini traversed the magnetopause and bow shock a few thousand times during the mission. At each of these crossings we can employ boundary models to

track from the crossing location back to the nose of the magnetosphere and in turn infer the upstream dynamic pressure which would place a boundary at that location (under steady state conditions). Jackman et al. (2019) explored this, utilising the magnetopause model of Kanani et al. (2010) and the bow shock model of Went et al. (2011). When searching for evidence of solar wind compression on the magnetosphere through indirect means, we can explore the boundary crossing intervals and take information from these inferred dynamic pressures. In particular, we can examine cases where Cassini's radial distance from the planet is increasing, and the spacecraft crosses the magnetopause outbound followed by the bow shock outbound next. If this inter-crossing interval (and associated magnetosheath residence time) is short, and/or the inferred dynamic pressure at these successive boundary crossings shows a large difference, it may reasonably be assumed that this corresponds to an interval where the magnetosphere was undergoing compression such that the bow shock was moved inward of its nominal position.
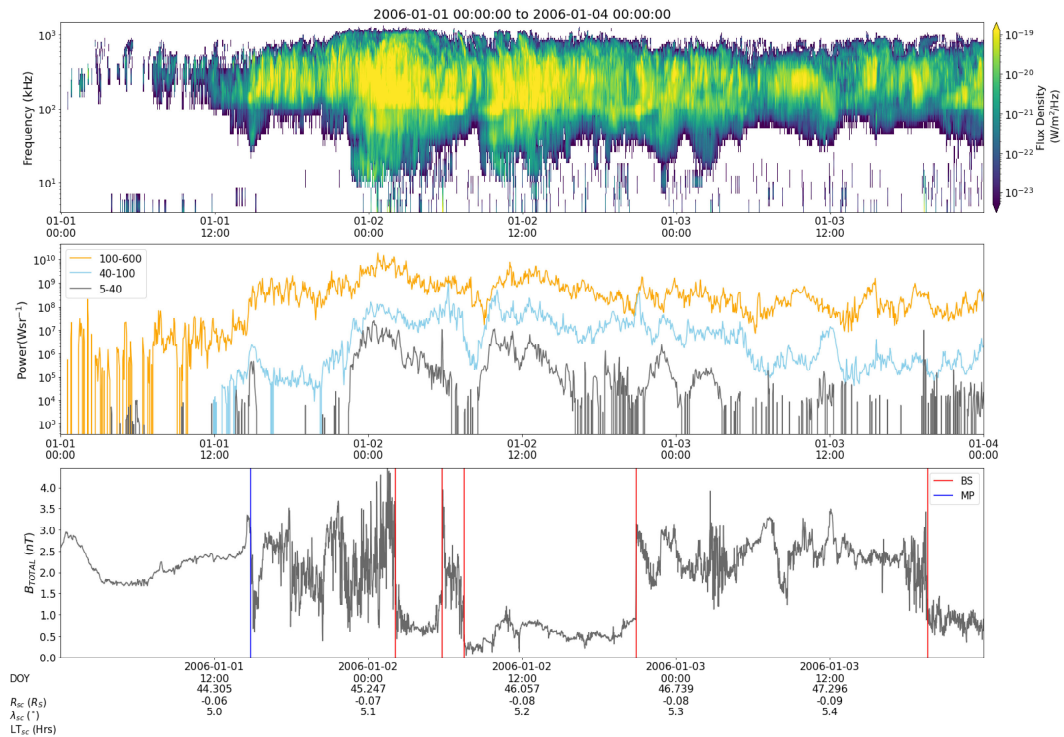
Figure 3: *A 3 day interval from 2006 day 001-004 (January 1st-4th) in the same format as Figure 2 with a radio spectrogram, integrated radio powers, and total magnetic field strength. Vertical lines on the bottom panel show the times of magnetopause (blue) and bow shock (red) boundary crossings.*

In Figure 3 we examine one such example and compare to the observed radio emissions. During the three-day interval shown, Cassini begins in the magnetosphere at a radial distance of ~ 44 R_S pre-dawn. At 14:49 on day 001, Cassini crossed the magnetopause outbound. Less than 12 hours later, at 02:07 on day 002, Cassini crossed the bow shock outbound. This outbound crossing was preceded by an interval of significantly enhanced

magnetosheath magnetic field amplitude. The inferred upstream dynamic pressure at these crossings was 0.022 and 0.19 nPa respectively. The latter value represents significantly compressed solar wind when compared to the typical distribution of solar wind dynamic pressure (D_P) values at the orbit of Saturn (Jackman & Arridge, 2011). The following bow shock crossings over the subsequent 30 hours show a slowly decreasing profile of D_P, with values of 0.178, 0.173, 0.138 and 0.101 nPa for the bow shock crossings marked by vertical lines on Figure 3. This interval of solar wind compression is tied closely to an extended SKR burst and associated "monster" LFE which began to build from ∼15:00 on day 001, with an order of magnitude increase in main SKR band power (middle panel), followed by an explosive ignition of the lower frequency components of the radio spectrum from ∼22:00 on day 001. This intense LFE then persisted for several planetary rotations, only petering out from early on day 003.

4   Conclusions and perspectives

In this article we have briefly summarised some of the key work linking Saturn's radio emissions to extreme upstream driving and significant magnetospheric dynamics. We have outlined several ways that our list (Jackman, 2022) of magnetopause and bow shock crossings from the Cassini mission can be used to select out extended solar wind intervals (for direct sampling, Section 3.1 above), and pairs of boundary crossings with large gradient in inferred solar wind dynamic pressure (indirect sampling, Section 3.2 above). Several open questions remain and below we list several, along with ideas for how they might be tackled in the near future:

- How is the lag time between a solar wind compression and radio response impacted by the observer location? Taubenschuss et al. (2006) examined the link between SKR and upstream parameters during the Cassini approach near dawn, when the steady local time viewing position was most favourable relative to the primary SKR beaming pattern. How can we use cases from the rest of the Cassini mission at other local times to test the response time to known compressions?

- Are long (multiple planetary rotation) LFEs a near-perfect proxy for compression? These "monster" LFEs (O'Dwyer et al., 2023) are seen from case studies (Bunce et al., 2005; Kurth et al., 2005; Palmerio et al., 2021) and small statistical studies (Jackman et al., 2009; Reed et al., 2018; Lamy et al., 2018) to almost universally link to extreme compression-driven magnetospheric dynamics, and to have a different character to the PPO-modulated shorter SKR bursts which appear far more frequently in the dataset. The work of O'Dwyer et al. will ultimately lead to a complete list of LFEs from the mission and this will enable quantification of the distribution of LFE durations, allowing us to explore if there is a threshold above which "long" LFEs have properties distinct from their shorter counterparts. A key element of this future work will be pinning down the timeline from solar wind compression to LFE appearance, cementing the links to the PPO modulations (Bradley et al., 2020), and thus clarifying each piece of the overarching physical scenario.

- What impact does observer position have on confidence in correlating radio behaviour and upstream driving? Lamy et al. (2009) built radio maps based on Cassini data from early in the mission (up until 2008) which showed that SKR sources are co-located with the UV main auroral oval, lying along a circumpolar oval at all local times, while Cecconi et al. (2009) noted that the magnetic footprint of these SKR sources covers 70° to 80° latitude in both hemispheres. From these source locations, the SKR emission is beamed along a thin hollow cone and the resulting observed pattern of emission is one where the SKR emission varies significantly with local time, with SKR power maximising in a several-hours-wide sector pre-dawn (peaking at 08:00 LT) (Reed et al., 2018). Lamy (2017) showed that, when observed remotely, the apparent emission angle of the SKR varies with frequency and also with time and/or observer location. In that work, they identify open questions about the variation of beaming angle around the magnetic field vector at the source, and the impact of refraction. What is certain is that the viewing geometry of the SKR is complex. The dynamics in so-called unfavourable viewing regions (such as near dusk) remain to be quantified, as case studies have indicated that the result of the beaming pattern can be a significant attenuation of LFEs in a particular local time sector. This has to be appropriately factored into our analysis of LFEs recurrence and temporal trends in radio power. We risk losing a vast amount of information from noon-to-midnight local times if we cannot find a way to appropriately account for poorer visibility in these regions.

- Which upstream parameters are most closely linked with the appearance of long LFEs? Future work will include the use of mutual information theory to compare upstream measures such as solar wind dynamic pressure, velocity, density and IMF magnitude with time series of integrated radio power across the lower frequency bands. Similar techniques have been employed at Earth to match the timescales for correlation of upstream metrics with geomagnetic indices, particularly during extreme substorm intervals.

- What is the spectral morphology of LFEs and what does this tell us about the vertical structure of the auroral acceleration region? Statistical analysis of SKR bursts and LFEs from the entire Cassini mission will soon be possible, based on the catalogue of O'Dwyer et al. (2023) and the results of using this catalogue as training data for a machine learning algorithm to select such events across 13 years. These approaches will provide the full shape of SKR bursts and how they evolve into LFEs via the motion of radio sources to higher altitude and the associated emission at lower frequencies. We wish to explore the timeline where a burst becomes an LFE to understand what is special about this lower frequency portion of Saturn's radio spectrum.

Acknowledgments

References

Andrews D. J., Coates A. J., Cowley S. W. H., Dougherty M. K., Lamy L., Provan G., Zarka P., 2010, Magnetospheric period oscillations at Saturn: Comparison of equatorial and high-latitude magnetic field periods with north and south Saturn kilometric radiation periods, *Journal of Geophysical Research (Space Physics)*, 115, A12252

Badman S. V., Cowley S. W. H., Lamy L., Cecconi B., Zarka P., 2008, Relationship between solar wind corotating interaction regions and the phasing and intensity of Saturn kilometric radiation bursts, *Annales Geophysicae*, 26, 3641

Bradley T. J., et al., 2020, Saturn's Nightside Dynamics During Cassini's F Ring and Proximal Orbits: Response to Solar Wind and Planetary Period Oscillation Modulations, *Journal of Geophysical Research (Space Physics)*, 125, e27907

Bunce E. J., Cowley S. W. H., Wright D. M., Coates A. J., Dougherty M. K., Krupp N., Kurth W. S., Rymer A. M., 2005, In situ observations of a solar wind compression-induced hot plasma injection in Saturn's tail, *Geophysical Research Letters*, 32, L20S04

Calvert W., 1981, The auroral plasma cavity, *Geophysical Research Letters*, 8, 919

Cecconi B., Zarka P., 2005, Model of a variable radio period for Saturn, *Journal of Geophysical Research (Space Physics)*, 110, A12203

Cecconi B., Lamy L., Zarka P., Prangé R., Kurth W. S., Louarn P., 2009, Goniopolarimetric study of the revolution 29 perikrone using the Cassini Radio and Plasma Wave Science instrument high-frequency radio receiver, *Journal of Geophysical Research (Space Physics)*, 114, A03215

Cecconi B., Witasse O., Jackman C. M., Sánchez-Cano B., Mays M. L., 2022, Effect of an Interplanetary Coronal Mass Ejection on Saturn's Radio Emission, *Frontiers in Astronomy and Space Sciences*, 9, 800279

Desch M. D., 1982, Evidence for solar wind control of Saturn radio emission, *Journal of Geophysical Research: Space Physics*, 87, 4549

Desch M. D., Rucker H. O., 1983, The relationship between Saturn kilometric radiation and the solar wind, *Journal of Geophysical Research: Space Physics*, 88, 8999

Dougherty M. K., et al., 2004, The Cassini Magnetic Field Investigation, *Space Science Reviews*, 114, 331

Ergun R. E., et al., 1998, FAST satellite wave observations in the AKR source region, *Geophysical Research Letters*, *25, 2061*

Galopeau P. H. M., Zarka P., Le Quéau D., 1995, Source location of Saturn's kilometric radiation: The Kelvin-Helmholtz instability hypothesis, *Journal of Geophysical Research: Space Physics*, *100, 26397*

Gurnett D. A., et al., 2004, The Cassini Radio and Plasma Wave Investigation, *Space Science Reviews*, *114, 395*

Jackman C., 2022, List of Saturn magnetopause and bow shock crossings by the Cassini spacecraft, doi:10.5281/zenodo.5913537, `https://doi.org/10.5281/zenodo.5913537`

Jackman C. M., Arridge C. S., 2011, Solar Cycle Effects on the Dynamics of Jupiter's and Saturn's Magnetospheres, *Solar Physics*, *274, 481*

Jackman C. M., Achilleos N., Bunce E. J., Cowley S. W. H., Dougherty M. K., Jones G. H., Milan S. E., Smith E. J., 2004, Interplanetary magnetic field at ∼9 AU during the declining phase of the solar cycle and its implications for Saturn's magnetospheric dynamics, *Journal of Geophysical Research (Space Physics)*, *109, A11203*

Jackman C. M., Achilleos N., Bunce E. J., Cowley S. W. H., Milan S. E., 2005a, Structure of the interplanetary magnetic field during the interval spanning the first Cassini fly-through of Saturn's magnetosphere and its implications for Saturn's magnetospheric dynamics, *Advances in Space Research*, *36, 2120*

Jackman C. M., Achilleos N., Bunce E. J., Cecconi B., Clarke J. T., Cowley S. W. H., Kurth W. S., Zarka P., 2005b, Interplanetary conditions and magnetospheric dynamics during the Cassini orbit insertion fly-through of Saturn's magnetosphere, *Journal of Geophysical Research (Space Physics)*, *110, A10212*

Jackman C. M., Lamy L., Freeman M. P., Zarka P., Cecconi B., Kurth W. S., Cowley S. W. H., Dougherty M. K., 2009, On the character and distribution of lower-frequency radio emissions at Saturn and their relationship to substorm-like events, *Journal of Geophysical Research (Space Physics)*, *114, A08211*

Jackman C. M., Thomsen M. F., Dougherty M. K., 2019, Survey of Saturn's Magnetopause and Bow Shock Positions Over the Entire Cassini Mission: Boundary Statistical Properties and Exploration of Associated Upstream Conditions, *Journal of Geophysical Research (Space Physics)*, *124, 8865*

Kaiser M. L., Desch M. D., 1984, Radio emissions from the planets earth, Jupiter, and Saturn., *Reviews of Geophysics and Space Physics*, *22, 373*

Kaiser M. L., Desch M. D., Warwick J. W., Pearce J. B., 1980, Voyager Detection of Nonthermal Radio Emission from Saturn, *Science*, *209, 1238*

Kanani S. J., et al., 2010, A new form of Saturn's magnetopause using a dynamic pressure balance model, based on in situ, multi-instrument Cassini measurements, *Journal of Geophysical Research (Space Physics)*, *115, A06207*

Kimura T., et al., 2013, Long-term modulations of Saturn's auroral radio emissions by the solar wind and seasonal variations controlled by the solar ultraviolet flux, *Journal of Geophysical Research (Space Physics)*, *118, 7019*

Kurth W. S., et al., 2005, An Earth-like correspondence between Saturn's auroral features and radio emission, *Nature*, *433, 722*

Lamy L., 2017, The Saturnian kilometric radiation before the Cassini Grand Finale, *in Planetary Radio Emissions VIII, eds Fischer G., Mann G., Panchenko M., and Zarka P.*, pp 171–190, doi:10.1553/PRE8s171

Lamy L., Zarka P., Cecconi B., Prangé R., Kurth W. S., Gurnett D. A., 2008a, Saturn kilometric radiation: Average and statistical properties, *Journal of Geophysical Research (Space Physics)*, *113, A07201*

Lamy L., Zarka P., Cecconi B., Hess S., Prangé R., 2008b, Modeling of Saturn kilometric radiation arcs and equatorial shadow zone, *Journal of Geophysical Research (Space Physics)*, *113, A10213*

Lamy L., Cecconi B., Prangé R., Zarka P., Nichols J. D., Clarke J. T., 2009, An auroral oval at the footprint of Saturn's kilometric radio sources, colocated with the UV aurorae, *Journal of Geophysical Research (Space Physics)*, *114, A10212*

Lamy L., et al., 2013, Multispectral simultaneous diagnosis of Saturn's aurorae throughout a planetary rotation, *Journal of Geophysical Research (Space Physics)*, *118, 4817*

Lamy L., et al., 2018, Saturn's Northern Aurorae at Solstice From HST Observations Coordinated With Cassini's Grand Finale, *Geophysical Research Letters*, *45, 9353*

Lamy L., Waters J., Louis C. K., 2023, Comparative visibility of planetary auroral radio emissions and implications for the search for exoplanets, *in Planetary, Solar and Helispheric Radio Emissions IX, eds Louis, C. K. and Jackman, C. M. and Fischer, G. and Sulaiman, A. H. and Zucca, P.*, DIAS and TCD, doi:10.25546/103091

Lecacheux A., Genova F., 1983, Source Localization of Saturn Kilometric Radio Emission, *Jounral of Geophysical Research: Space Physics*, *88, 8993*

Morioka A., et al., 2007, Dual structure of auroral acceleration regions at substorm onsets as derived from auroral kilometric radiation spectra, *Journal of Geophysical Research (Space Physics)*, *112, A06245*

Nakamura Y., et al., 2019, Seasonal variation of north-south asymmetry in the intensity of Saturn Kilometric Radiation from 2004 to 2017, *Planetary and Space Science*, *178, 104711*

O'Dwyer E., Jackman C. M., Domijan K., Lamy L., Louis C. K., 2023, Selection of low frequency extensions of Saturn Kilometric Radiation, *in Planetary, Solar and Heliospheric Radio Emissions IX, eds Louis, C. K. and Jackman, C. M. and Fischer, G. and Sulaiman, A. H. and Zucca, P.*, DIAS and TCD, doi:10.25546/103103

Palmerio E., et al., 2021, Magnetic Structure and Propagation of Two Interacting CMEs From the Sun to Saturn, *Journal of Geophysical Research (Space Physics)*, *126, e2021JA029770*

Reed J. J., Jackman C. M., Lamy L., Kurth W. S., Whiter D. K., 2018, Low-Frequency Extensions of the Saturn Kilometric Radiation as a Proxy for Magnetospheric Dynamics, *Journal of Geophysical Research (Space Physics)*, *123, 443*

Rucker H. O., et al., 2008, Saturn kilometric radiation as a monitor for the solar wind?, *Advances in Space Research*, *42, 40*

Taubenschuss U., Rucker H. O., Kurth W. S., Cecconi B., Zarka P., Dougherty M. K., Steinberg J. T., 2006, Linear prediction studies for the solar wind and Saturn kilometric radiation, *Annales Geophysicae*, *24, 3139*

Thomsen M. F., Jackman C. M., Lamy L., 2019, Solar Wind Dynamic Pressure Upstream From Saturn: Estimation From Magnetosheath Properties and Comparison With SKR, *Journal of Geophysical Research (Space Physics)*, *124, 7799*

Warwick J. W., et al., 1981, Planetary Radio Astronomy Observations from Voyager 1 near Saturn, *Science*, *212, 239*

Went D. R., Hospodarsky G. B., Masters A., Hansen K. C., Dougherty M. K., 2011, A new semiempirical model of Saturn's bow shock based on propagated solar wind parameters, *Journal of Geophysical Research (Space Physics)*, *116, A07202*

Young D. T., et al., 2004, Cassini Plasma Spectrometer Investigation, *Space Science Reviews*, *114, 1*

Zarka P., Lamy L., Cecconi B., Prangé R., Rucker H. O., 2007, Modulation of Saturn's radio clock by solar wind speed, *Nature*, *450, 265*